Erschienen in: ACS Nano ; 10 (2016), 11. - S. 10041-10048
http://dx.doi.org/10.1021/acsnano.6b04677

ACSNANO

www.acsnano.org

ARTICLE

Passing Current through Electrically Conducting Lyotropic Liquid Crystals and Micelles Assembled from Hybrid Surfactants with π-Conjugated Tail and Polyoxometalate Head

Alexander Klaiber and Sebastian Polarz*

Functional Inorganic Materials Lab, Department of Chemistry, University of Konstanz, Universitaetsstrasse 10, 78457 Konstanz, Germany

Supporting Information

ABSTRACT: The solvent-mediated ability for molecularly encoded self-assembly into states of higher order (micelles, lyotropic liquid crystals) embodies the basis for many applications of surfactants in science and society. Surfactants are used frequently in recipes for nanoparticle synthesis. Because ordinary surfactants comprise insulating constituents (alkyl groups as side-chains and charged organic heads), such nanostructures are wrapped in an electrically inactive barrier, and this is a large disadvantage for future developments in nanotechnology. Implications of micelles with electrically conducting walls made from either "metallic" or "semiconducting" surfactants are huge, also in other areas such as nano-electrocatalysis or micellar energy storage. We cross this frontier by replacing not only the hydrophilic chain but also the hydrophilic head by electronically conducting entities. We report the synthesis of surfactants with oligo *para*-phenylene-ethynylene as a π-conjugated side-chain attached to a redox-active, inorganic polyoxometalate cluster as charged head. It is proven that electronic communication between head and tail takes place. Hybridization on the molecular level leads to the emergence of advanced surfactant features such as semiconductor properties (E_{gap} = 2.6 eV) in soft lyotropic systems (micelles, liquid crystals).

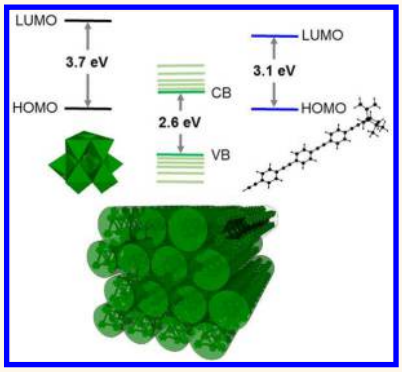

KEYWORDS: *surfactants, liquid crystals, polyoxometalates, organic−inorganic hybrids, molecular conductors*

Molecular architectonics, the assembly of molecular entities into functional patterns coupling their properties to the nano-, then to the meso-, and finally to the macroscopic world, is key for implementing future technologies.[1,2] Eventually, the spontaneous formation of such organized structures takes place as an intrinsic property of a system containing discrete constituents, a process termed self-assembly.[3,4] A special class of self-assembling materials are liquid crystals (LCs), because they unify structural order and a high degree of mobility. This leads to a plethora of properties as also stated in the seminal article published by Tschierske in 2013.[5] Liquid crystals are formed by certain molecular compounds, and one can distinguish between thermotropic and lyotropic LCs.

Rising interest was devoted to the self-assembly of π-conjugated systems because of their large potential in (supra)molecular electronics.[6] A prominent application is for instance in field-effect transistors.[7] Several papers have also reported on the semiconducting features of LC phases formed by these molecules.[8,9] This year (2016) Kim and co-workers have summarized the potential of LCs based on graphene oxide.[10] Most of the described systems belong to thermotropic phases. A molecular system with lyotropic (solvent-triggered self-assembly) and amphiphilic properties in combination with electronic conductivity could feature very interesting properties, for example, micelles as nanoreactors with electrically active and transmittive shells. Another important aspect is that surfactants located on the surfaces of nanoparticles lead to an insulating layer. This is a large disadvantage for numerous applications of nanoparticles requiring electronic transport.[11]

Little is known about electrically conducting surfactants or amphiphiles in general. Li and co-workers presented in an interesting study a molecular hybrid of fullerene attached to a polythiophene oligomer. They showed some amphiphilic

Received: July 13, 2016
Accepted: November 3, 2016
Published: November 3, 2016

DOI: 10.1021/acsnano.6b04677
ACS Nano 2016, 10, 10041−10048

properties.[12] Hecht and co-workers achieved a *meta*-phenylene ethynylene derivative bound to an oligo-ethylene oxide chain as a hydrophilic constituent of the amphiphile. The authors reported intriguing, helical self-assembly.[13] For an amphiphile, or finally a surfactant, appointed for molecular electronics, it becomes clear that the isolating character of typical, hydrophilic headgroups such as oligo-ethylene-oxide or ammonium is a large disadvantage. Therefore, a class of surfactants comprising a hydrophobic and electrically conducting chain and a (hydrophilic) headgroup, which is also capable of conducting electrons, would represent a major advance.

Recently, organic–inorganic hybrid surfactants with heads containing transition metal species were receiving attention because of their ability to self-assemble could be combined with added properties characteristic for coordination compounds (magnetic properties, catalytic activity, *etc.*).[14] Our group could identify a surfactant class with a pure inorganic head, namely, a lacunary polyoxometalate (POM) cluster $[PW_{11}O_{39}]$, and conventional alkyl chains as hydrophobic moieties.[15−19] From our previous work we know the polytungstate head can be reduced (for example by electrochemical methods),[18] and, in addition, reduced POMs belong to compounds with partially delocalized electronic systems (Robin–Day classification II).[20] Thus, $[PW_{11}O_{39}]$ is a promising candidate for the desired, electrically conducting headgroup. Obviously the alkyl chain needs to be exchanged by a conducting entity, *e.g.*, a π-conjugated system. Others have already shown the attachment of POM species to π-systems such as dyes (for example, perylene) can be done in general, but their target was not the synthesis of surfactant species.[21−24] Therefore, in our current contribution, we would like to create a compound with surfactant-like architecture containing a linear, π-conjugated chain as used in molecular electronics with a terminal, hydrophilic POM cluster.

RESULTS AND DISCUSSION

Surfactant Preparation. The target compound (**3**), also noted as PW_{11}TPE, a lacunary $[PW_{11}O_{39}]$ polytungstate cluster attached to two *para*-phenylene ethynylene trimers *via* siloxane bridges, was synthesized as depicted in Scheme 1.

Scheme 1. Synthesis of the amphiphilic compound with an inorganic polytungstate head and π-conjugated side chain.

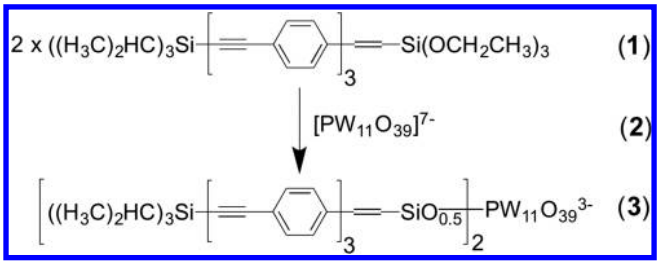

The alkoxy-silane-modified *para*-phenylene ethynylene derivative (**1**) required for coupling with the lacunary POM cluster and its synthesis are described in detail in Supporting Information Figure S-1. The successful reaction of **1** with $[PW_{11}O_{39}]^{7-}$ (**2**) was examined by various methods (see also Supporting Information Figure S-2), but most importantly using ^{183}W-nuclear magnetic resonance (NMR) spectroscopy and electrospray ionization mass spectrometry (ESIMS) shown in Figure 1.

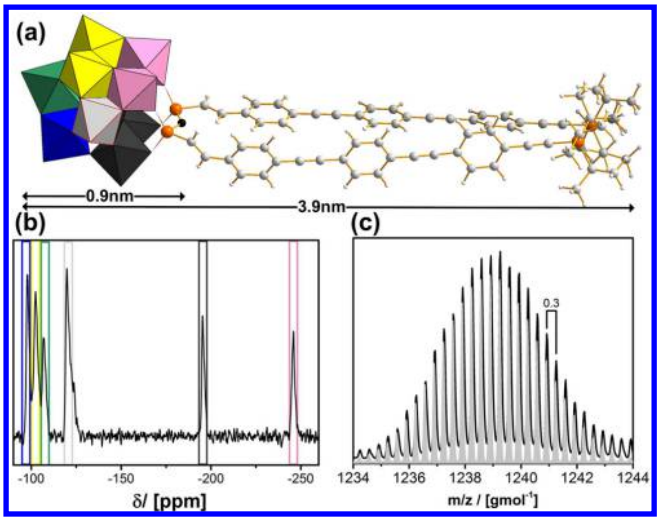

Figure 1. (a) Molecular structure of compound 3 as proven from various analytical data. The color code of the $[PW_{11}O_{39}]$ headgroup marks the symmetry equivalent W atoms appearing in the ^{183}W NMR spectroscopy (b). (c) Experimental ESIMS pattern (black) in comparison to the calculated pattern of the molecular ion 3 (gray).

The isotope lines of the ESIMS signal centered at m/z = 1239 g mol^{-1} and recorded in negative ion mode are separated by 0.33 unit, affirming the charge of the ion is −3. Thus, the resulting mass of the molecular species ($m \times z$ = 3717 g mol^{-1}) matches nicely the nonfragmented molecular ion **3**, and as a result, there is a perfect match with the theoretically expected isotope pattern (Figure 1c). In the ^{183}W NMR spectrum shown in Figure 1b one sees the characteristic 2:2:1:2:2:2 pattern of the lacunary $[PW_{11}O_{39}]$ POM cluster bound to two organo-siloxane units. Thus, one can infer the molecular architecture is intact. Also in the ^{31}P NMR spectroscopy (Figure S-2b) one sees only one signal (δ = −13.94), which is characteristic for the central "PO_4" unit in $[PW_{11}O_{39}]$ and proves the high purity of the compound. FT-IR spectroscopy (Figure S-2a) confirms the latter results, and it can be seen that also the CC triple bonds are still present ($\tilde{\nu}$ = 2150 cm^{-1}). The presence of the characteristic Si–O–Si vibration ($\tilde{\nu}$ = 1110 cm^{-1}) is also in full agreement with the proposed structure of the surfactant. Therefore, the molecular structure of the target compound is proven unambiguously.

Investigation of Self-Organization. Similar to the alkyl-modified $[PW_{11}O_{39}]$ surfactants (for example $(CH_3(CH_2)_{14}CH_2SiO_{0.5})_2[PW_{11}O_{39}]^{3-}$ (**4**) as a reference; all reference systems used in this study are summarized in Supporting Information Figure S-3),[15−19] we also expect that compound **3** has amphiphilic properties because of its dipolar character considering the hydrophilic and charged headgroup and (two) attached, hydrophobic hydrocarbon chains. Water is added to **3**, and for concentrations c > 1 g/L one still observes a sediment remaining in the test vial. This indicates the solubility of **3** is lower compared to classical organic surfactants, *e.g.*, SDS (sodium dodecyl sulfate), and also the alkyl analogue **4**. However, even at c = 0.1 g/L we could observe the formation of self-assembled structures in water (see Figure 2). In particle size distribution functions obtained from dynamic light scattering (DLS) one sees two signals at a hydrodynamic diameter D_H = 4.9 and 18 nm (Figure 2a).

The critical micelle concentration (CMC) of surfactants such as SDS (CMC = 2.3 g/L) or polysorbate 80 (CMC = 0.16 g/L)

DOI: 10.1021/acsnano.6b04677
ACS Nano 2016, 10, 10041−10048

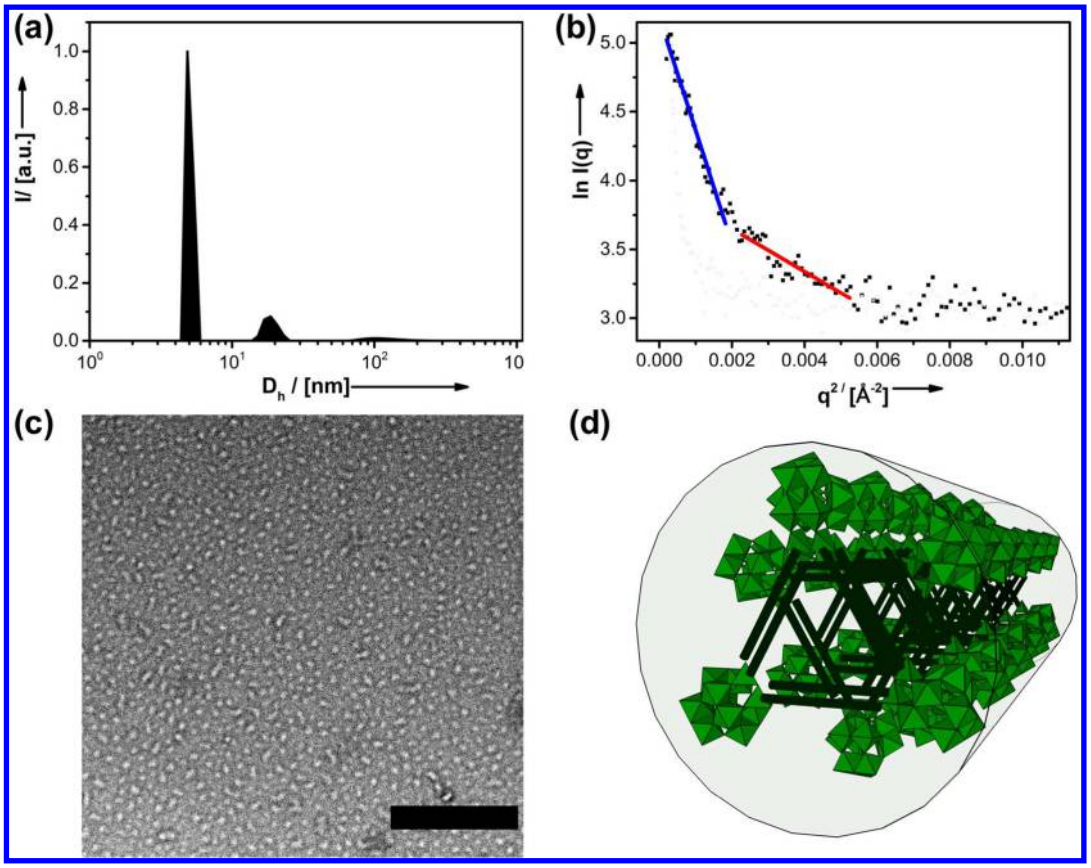

Figure 2. (a) Particle size distribution curve obtained from DLS measurements. (b) Guinier plot of SAXS data: gray circles ≅ background measurement; black squares ≅ 3 in aqueous solution; blue, red line ≅ linear fits for $D_{G1,2}$. (c) TEM micrograph of a dispersion of aggregates formed by 3 in aqueous solution; scale bar = 500 nm. Larger TEM micrographs are given in Supporting Information Figure S-4. (d) Proposed structure of the aggregates: green ≅ polyhedral plot of the $[PW_{11}O_{39}]^{3-}$ headgroup; black ≅ organic phenylene ethynylene chains. Cations are omitted. All dispersions had a concentration of 0.1 g/L of PW_{11}TPE (3) in water.

is typically larger. Attempts to determine the CMC of PW_{11}TPE precisely were not successful, because ring tensiometry fails for all surfactants with highly charged PW_{11} heads[25] and other methods (such as DLS) are no longer sensitive to such low concentrations (<0.1 g/L). The overall lower solubility and lower critical aggregation concentration are assigned to the presence of the π-conjugated chain, which could induce other, stronger intermolecular interactions in the hydrophobic block such as $\pi-\pi$ bonding. For further clarification, we have performed small-angle X-ray scattering (SAXS) measurements. Considering the Kratky plot of the SAXS data (see Supporting Information Figure S-4), the shape of the observed aggregates is close to a rigid-rod morphology, indicated by the linear increase of the curve. Further, the dimension of the aggregates is $D_{G1} \approx 6$ nm and $D_{G2} \approx 20$ nm according to the two different slopes obtained from the Guinier analysis of the data (Figure 2b), which fits nicely with the values obtained from DLS. Images received from transmission electron microscopy (TEM) analysis (Figure 2c) are consistent with the latter results. The impression of "hollow structures" is typical for self-assembled structures resulting from $[PW_{11}O_{39}]$ surfactants due to the large difference in electronic density between the headgroup region and the organic tail.[15,17] Although there is a large tendency for film formation, the size distribution of the objects is narrow and the objects are slightly elongated with dimensions of ~15−20 nm. Compared to alkyl-modified surfactants, for example the reference system **4**, there are some important differences. D_H = 4.9 nm is obviously smaller than the double extension of PW_{11}TPE (see Figure 1a), and this speaks for a substantial interdigitation of the hydrocarbon chains. Because the hydrocarbon chain can adopt only a stretched conformation because of the triple bonds, interdigitation is problematic since intersection becomes almost unavoidable for any classical shape of a micelle. However, density functional calculations show that the two phenylene ethynylene chains do not prefer a parallel orientation, but there is an angle between them of ~60° (see Supporting Information S-5). Considering this specific geometry of the amphiphile **3**, we propose the special structure of the micellar aggregates shown in Figure 2d. Our suggestion is in line with the crystal structure of a lacunary Dawson polyoxometalate cluster bound to a pyrene moiety.[23] The model also accounts for the elongated shape of the aggregates, which could be a result of the additional $\pi-\pi$ interactions of the phenylene ethynylene moieties. It is important to note that all structures involving charged surfactants contain substantial amounts of counterions. For surfactants with polyoxometalate heads this aspect is crucial because of the high negative charge. We have recently explored polyoxotungstate surfactants with charges up to −5, and we saw that not only the choice of cation is important but also surfactants with charges higher than −3 exhibit unusual self-assembly features because of the inevitable electrostatic repulsion.[25] Here, we have not varied the counterion. Sodium compounds were used in all cases. We assume that hydrated Na^+ remains in close proximity to the

DOI: 10.1021/acsnano.6b04677
ACS Nano 2016, 10, 10041−10048

negative headgroup, but the exact position cannot be resolved as for other systems known in the literature.[26−28]

The self-assembly at high concentration of PW_{11}TPE (lyotropic LC) was studied using SAXS and TEM given in Figure 3. The water content in the samples was determined by thermogravimetric analysis and was found to be 4.7%. At low angles, two diffraction signals are present, which fit to a hexagonally ordered cylindrical liquid crystal phase (a = 4.99 nm) (space group P_{6mm}). In addition, there is one signal at higher q values (c = 1.14 nm), which we assign to a dense packing of the $[PW_{11}O_{39}]$ headgroups located at the surface of the cylindrical aggregates (see Figure 3a).

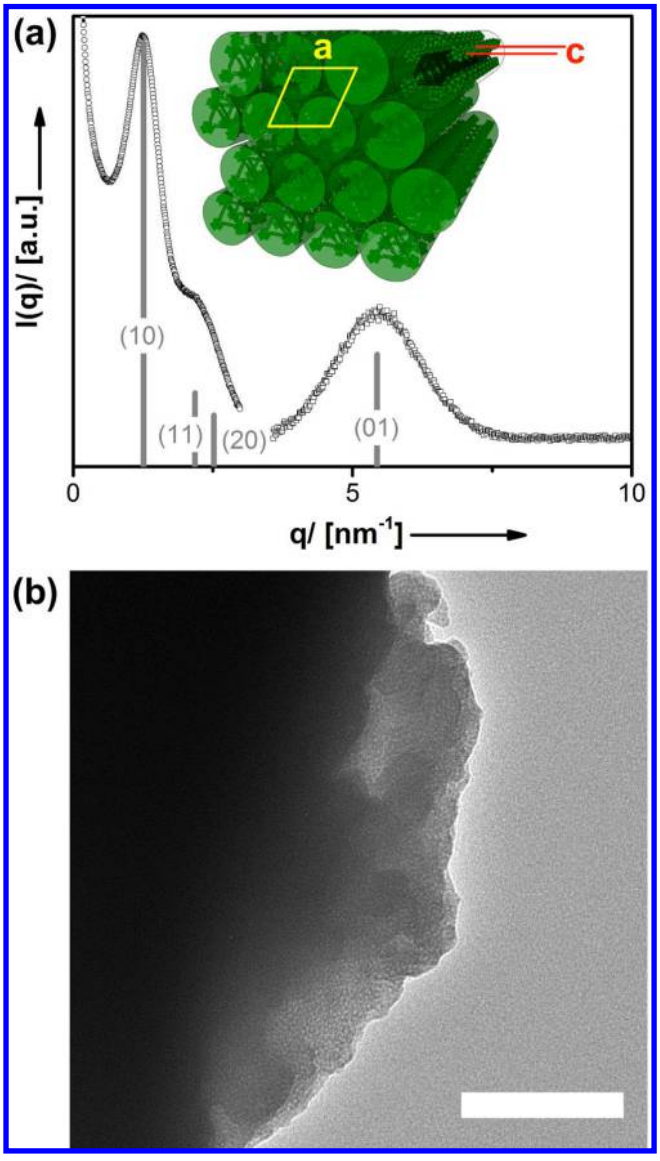

Figure 3. (a) Experimental small-angle X-ray (Cu Kα) diffraction pattern measured at two different detector distances (circles, squares) and signals expected (gray bars) for a hexagonal packing of cylinders (P_{6mm}) with periodicity a and for an additional dense packing of the headgroups in the single cylinders c. (b) TEM micrograph of solid, dried PW_{11}TPE; scale bar = 100 nm.

However, the internal order is not high, which is signaled by the significant width of the SAXS signals. The latter is confirmed by TEM investigations, for which we could only find a disordered, wormlike phase (Figure 3b). Compared to the alkyl derivative as a reference ($PW_{11}C_{16}$),[15] performing electron microscopy is intricate because PW_{11}TPE undergoes radiation damage much more easily.

Investigation of Electronic and Electrical Properties. Now that the amphiphilic properties of PW_{11}TPE (**3**) have been examined and some self-assembled structures have been introduced, the question needs to be answered, if there is any electronic communication between the redox-active $[PW_{11}O_{39}]$ headgroup and the π-conjugated chain(s). We studied the electronic properties of **3** in solution first. As the solubility of PW_{11}TPE is limited in water, electrical (cyclic voltammetry (CV)) and electronic (UV/vis and photoluminescence (PL)) characterization was carried out in organic solvents for better comparison to references ($PW_{11}C_{16}$, PW_{11}, and TPE) and to meet the required minimal concentrations for the analytical techniques. Figure 4a shows cyclic voltammetry data of PW_{11}TPE in comparison to the alkyl analogue $PW_{11}C_{16}$.

Both compounds show two reduction/oxidation waves due to the redox pair W^{VI}/W^{V}. Two effects can be seen. The reversibility of the redox process is limited for $PW_{11}C_{16}$, as documented by the second oxidation wave in comparison to the corresponding reduction wave. Interestingly, for PW_{11}TPE the redox reversibility has increased significantly. Further, the reduction waves have shifted to lower potentials (−840 to −750 mV), meaning the transfer of one electron to the headgroup is eased.

It can be reasoned there is clearly an effect of the π-conjugated chain attached to the $[PW_{11}O_{39}]$ headgroup. Photoluminescence measurements also show an influence of the attached π-conjugated chain (Figure 4b). Whereas there is no or only limited signal for PW_{11} (**2**) and $PW_{11}C_{16}$ (**4**), the presence of the TPE chain leads to a noticeable fluorescence signal in the VIS region. Attaching the $[PW_{11}O_{39}]$ moiety to the TPE chain induces a red-shift of the fluorescence by $\Delta\lambda_{max}$ = 18 nm. From fluorescence lifetime measurements (Figure 4c) one sees there is clearly a biexponential decay for PW_{11}TPE and the related relaxation constants are markedly different (see fits given in Supporting Information Figure S-6). Because the electronic system of $[PW_{11}O_{39}]$ is very different from the organic TPE chain, it is expected that disparate decay constants exist. Because excitation is based on the adsorption band of TPE, the occurrence of both decays is an indication of the successful transfer of the excited state from the chain to the headgroup. The bare TPE chain (for better comparison also fitted by a biexponential curve) compares well to the slower decay rate of PW_{11}TPE, and the second component is much faster. Since it is known that fluorescence lifetimes are influenced by the presence of heavy atoms, the latter results can be interpreted as an additional evidence for the delocalization of the photogenerated, excited state from the π-conjugated chain to the polyoxometalate headgroup containing the heavy W atoms. We wanted to gain further, independent confirmation of the latter by using spectroelectrochemical (SEC) IR measurements (see Supporting Information Figure S-7). We expected a shift of the C≡C stretching vibration because of the occupation of antibonding orbitals, when an electron of a reduced $[PW_{11}O_{39}]$ headgroup would eventually hop to the π-conjugated chain. Clearly there is no shift, and as a result, one has to assume the transfer of electrons from the headgroup to the chain in solution is at least aggravated. Several factors can be responsible for this: First, one has to consider the reduction of conjugated π-systems is in general not favorable.[29] Then, in solution rotation of the chain

DOI: 10.1021/acsnano.6b04677
ACS Nano 2016, 10, 10041−10048

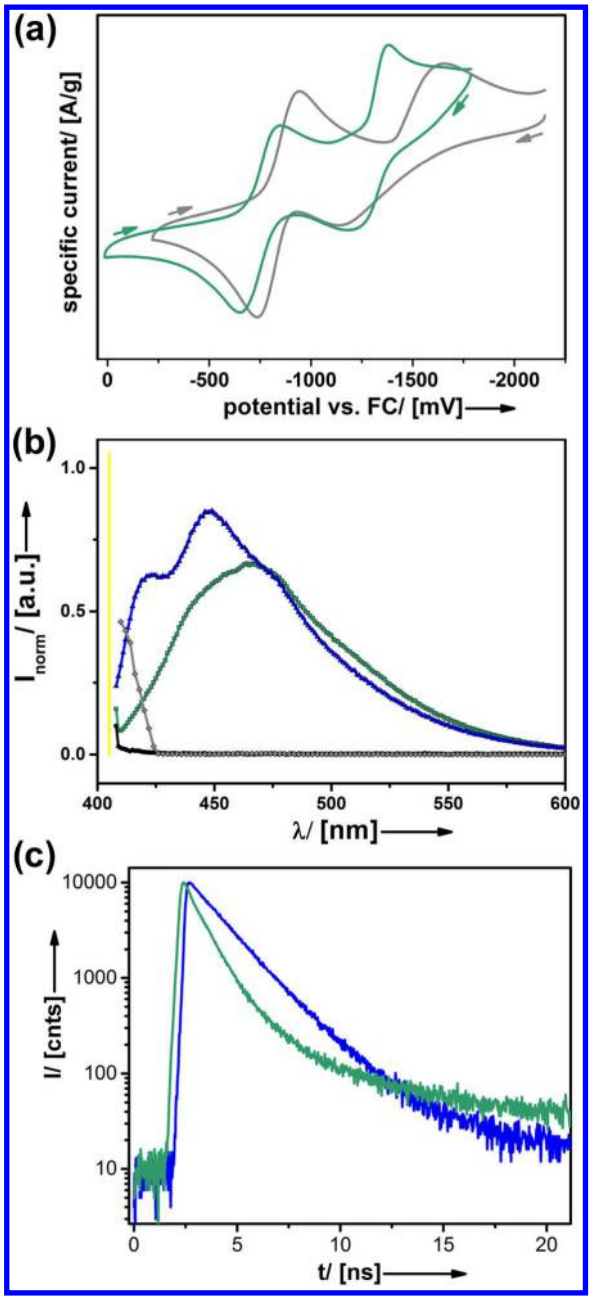

Figure 4. (a) CV data of $PW_{11}TPE$ (3) (green line) in comparison to $PW_{11}C_{16}$ (4) as a reference (gray line). (b) PL spectra of $PW_{11}TPE$ (3) (green squares) and as references PW_{11} (2) (black circles), $PW_{11}C_{16}$ (4) (gray hashes), and TPE (5) (blue triangles). The yellow line marks the excitation wavelength λ_{exc} = 405 nm. (c) Fluorescence decay curves for $PW_{11}TPE$ (3) (green line) in comparison to TPE (5) (blue curve).

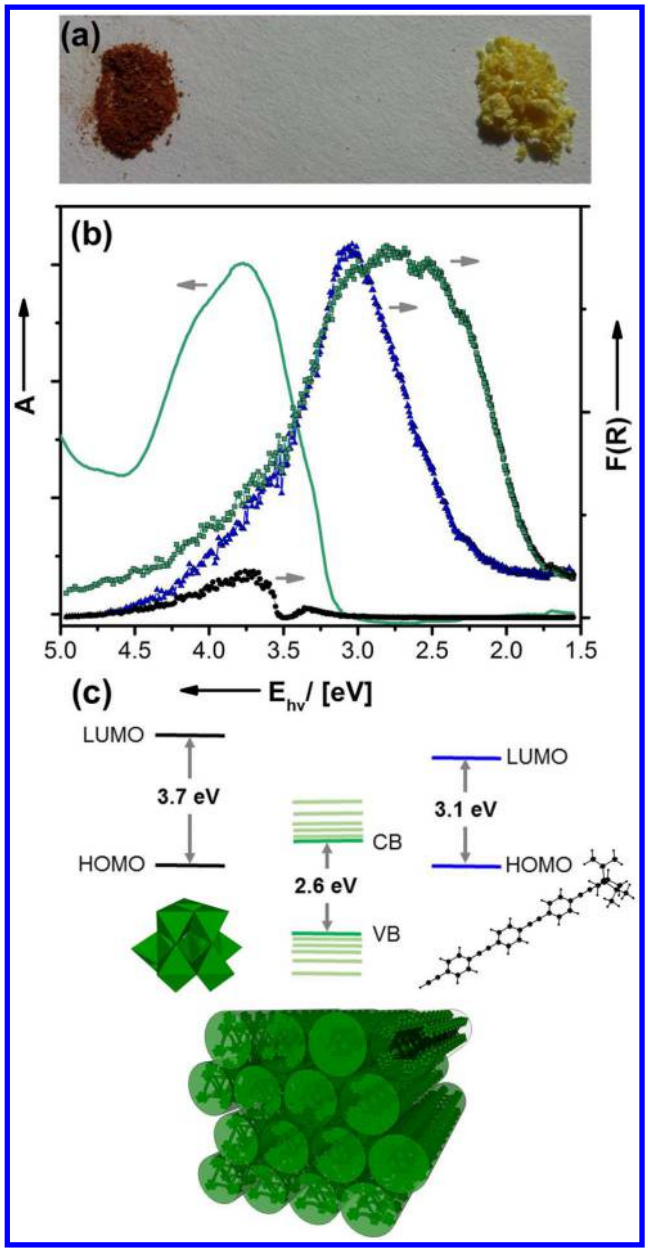

Figure 5. (a) Photographic images of $PW_{11}TPE$ (left) and the unmodified TPE chain (right). (b) UV/vis spectra of 3 in the solid state (green squares) and as references solid TPE (blue triangles) and $[PW_{11}O_{39}]Na_7$ (black circles) with $F(R) \cong$ Kubelka–Munk function. The absorption spectrum of 3 in solution is shown as well (green line). (c) By attachment of the lacunary $[PW_{11}O_{39}]$ cluster (left) to the TPE chain (right), one obtains a liquid crystalline semiconductor (middle) with a band gap in the visible range.

about the Si–C_{sp2} bond is possible, and therefore the chances for overlap between the head and the π-system are reduced.

Therefore, it makes sense to investigate the described solid-state structure of **3** next. As expected, it can be seen that "bare" TPE is a yellow compound with an adsorption maximum at λ_{max} = 399 nm ($E_{h\nu}$ = 3.1 eV). The "bare" $[PW_{11}O_{39}]$ also absorbs in the UV (Figure 5). Considering a "particle in a box model", the significant red-shift of the absorption band of PW_{11}OTPE compared to TPE can be explained by an extension of the electronic system. Further, one sees the band of **3** is significantly broader, and this is indicative for a bigger dispersion of the density of states (DOS) function. This and the fact that the optical properties of **3** in solution differ so much suggest that $PW_{11}TPE$ in its solid state has less molecular character and is gaining semiconducting properties. As a result, charge carriers can be delocalized over dimensions larger than just the molecular scale. This theory is confirmed by PL measurements shown in Supporting Information Figure S-8. While pure TPE (**5**) is characterized by several distinct fluorescence features, all signals are quantitatively quenched for **3**. We explain this by the increased delocalization of the excited state also to the headgroup region and fluorescence quenching because of the high atomic number of W, in addition to the

DOI: 10.1021/acsnano.6b04677
ACS Nano 2016, 10, 10041–10048

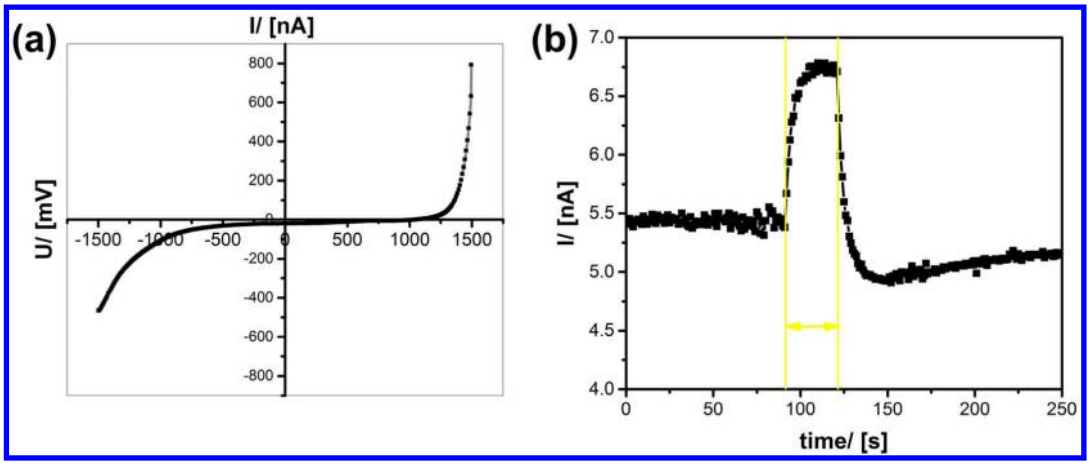

Figure 6. (a) I/V and (b) photocurrent measurement for PW_{11}TPE. The period when the material was exposed to light is marked by the yellow bars.

known "self-quenching" effect, due to excimer formation in high-concentration samples.[30]

Final proof that PW_{11}TPE truly is a semiconductor comes from current−voltage measurements and from testing the materials as a photoconductor (Figure 6). One sees that PW_{11}TPE shows the typical I/V behavior of semiconductors. The asymmetry in the graph (Figure 6a) is presumably due to the possible redox process (reduction of the head; see above). When PW_{11}TPE is irradiated with light, because of its semiconducting character, excitons (electron−hole pairs) are formed, and this increases the electrical conductivity of the material. Therefore, we can note an increase in current that quickly ceases when the light is turned off. Interestingly, afterward the resistance seems to be slightly higher than before but then recovers over time. When considering the results from PL and photosensor experiments together, it gets obvious that very interesting semiconducting properties arose from the presented hybrid material in LC phase. The determined band gap of 2.6 eV is very similar to established semiconductors such as ZnSe (2.7 eV), which opens the door for manifold applications.

CONCLUSIONS

In the current paper not only do we show that π-conjugated systems can be used for constructing soft semiconductors *via* thermotropic liquid crystals, but the presented organic−inorganic hybrid amphiphile allows entering the world of lyotropic, soft semiconductors. Because the set of analytical techniques is different for the micellar state and the LLC phase, it is very hard to compare the results directly. But it was shown that the type of aggregation also has an influence on the degree of electronic delocalization. When there is less conformational freedom of the π-conjugated chain with respect to the polyoxometalate head (in the solid state), delocalization is improved. It has also been demonstrated that in condensed phases intermolecular charge transfer between adjacent surfactants is possible and that this contributes to the semiconductor features.

When imagining possible applications of our materials, a first idea is to relate to classical semiconductors with similar gap energy (*e.g.*, ZnSe).[31,32] However, compared to semiconductor quantum dots, a soft semiconductor like that presented here is fundamentally different. Therefore, our system should not be seen as an alternative to inorganic nanoparticles. It is much more promising to identify possibilities benefiting from the features of the presented system. These are the surfactant characteristics and the presence of the polyoxometalate group. Tempting ideas are to use conducting surfactants for surface stabilization of nanoparticles, enabling direct interparticle charge transfer, or to explore the option for the generation of self-organizing photovoltaic films. In combination with the idea of electrically conducting micelles and considering the catalytic activity of heteropolyoxometalates we want to approach innovative routes in electrocatalysis. When redox-active compounds are confined in micelles with conductive walls, one can also imagine finding possible applications in energy storage by charge storage and transport *via* reduction and oxidation. However, before these perspectives can be realized, most importantly the solubility in water has to be improved, for example by attaching side-chains to the π-backbone. In addition, more advanced physical measurements are planned to understand the mechanism of charge generation and transport in these systems.

METHODS

General Information. All experiments involving Pd complexes were carried out under a nitrogen atmosphere using standard Schlenk techniques. Solvents were dried and distilled prior to use. Unless otherwise specified, reagents were used as received without further purification. Refer to Supporting Information Figure S-1 regarding numbering of compounds.

Synthesis of ((4-Iodophenyl)ethynyl)trimethylsilane (ii). A solution of 13.2 g (40 mmol) of 1,4-diiodobenzene (i), 1 mol % $Pd(PPh_3)_4$, 2 mol % CuI, and 50 mmol of trimethylsilylacetylene (TMSA) in 90 mL of tetrahydrofuran (THF)/NEt_3 (2:1, v/v) was prepared. After stirring for 20 h at 50 °C the solvent was evaporated and the residue was extracted with pentane. After evaporation of the solvent, the crude product was purified by column chromatography on silica gel and pentane as eluent. ^{1}H NMR (400 MHz, $CDCl_3$): δ (ppm) = 7.72−7.54 (m, 2H), 7.21−7.10 (m, 2H), 0.25, (s, 9H, TMS).

General Procedure for the Pd-Catalyzed Coupling of Terminal Alkynes and (ii). A solution of (ii), 1 mol % $Pd(PPh_3)_4$, 2 mol % CuI, and 1.05 equiv of terminal alkyne were prepared in THF/NEt_3 (2:1, v/v). After stirring for 20 h at 50 °C the solvent was evaporated and the residue was extracted with pentane. After evaporation of the solvent, the crude product was purified by column chromatography on silica gel and pentane as eluent.

Trimethylsilyl-protected Tri-iso-propylsilylacetylenyl Phenylacetylene (TMS-iii): colorless oil; yield 85%; ^{1}H NMR (400 MHz, $CDCl_3$) δ (ppm) = 7.39 (s, 4H, Ph), 1.13 (m, 21H, TIPS), 0.25 (s, 9H, $SiMe_3$).

DOI: 10.1021/acsnano.6b04677
ACS Nano 2016, 10, 10041−10048

Trimethylsilyl-protected Tri-iso-propylsilylacetylenyl bis-phenyl-acetylene (TMS-iv): yellowish powder; yield 91%; ^{1}H NMR (400 MHz, $CDCl_3$) δ (ppm) = 7.45 (m, 8H, both Ph), 1.14 (m, 21H, TIPS), 0.26 (s, 9H, $SiMe_3$).

Trimethylsilyl-protected Tri-iso-propylsilylacetylenyl tris-phenyl-acetylene (TMS-v): yellowish powder; yield 77%; ^{1}H NMR (400 MHz, $CDCl_3$) δ (ppm) = 7.50 (s, 4H, Ph) and 7.46 (m, 8H, 2×Ph), 1.14 (m, 21H, TIPS), 0.26 (s, 9H, $SiMe_3$).

General Procedure for the Selective Cleavage of the Trimethylsilyl Group. TMS-protected alkyne was dissolved in 240 mL of CH_2Cl_2/MeOH (1:2, v/v), and 15 equiv of K_2CO_3 was added. After stirring the resulting dispersion for 2 h, 240 mL of water was added. After separation of the phases, the organic solvent was removed. The obtained product was used without further purification.

(iii): white powder; yield 92%; ^{1}H NMR (400 MHz, $CDCl_3$) δ (ppm) = 7.42 (s, 4H, Ph), 3.15 (s, 1H, C≡CH), 1.13 (m, 21H, TIPS).

(iv): white powder; yield 87%; ^{1}H NMR (400 MHz, $CDCl_3$) δ (ppm) = 7.47 (s, 4H) and 7.45 (s, 4H, both Ph), 3.18 (s, 1H, C≡CH), 1.14 (m, 21H, TIPS).

(v): yellowish powder; yield 95%; ^{1}H NMR (400 MHz, $CDCl_3$) δ (ppm) = 7.51 (s, 4H, Ph), 7.48 (s, 4H, Ph at terminal alkyne), 7.46 (s, 4H, Ph at TIPS), 3.18 (s, 1H, C≡CH), 1.14 (s, 21H, TIPS); ^{13}C NMR (101 MHz, $CDCl_3$) δ (ppm) = 132.26, 132.16, 131.74, 131.73, 131.64, and 131.54 (aromatic CH), 123.75, 123.64, 123.30, 123.08, 122.97, and 122.28 (quaternary C's of Ph), 106.75 (C≡*C*−Si), 93.17 (C≡C−Si), 91.30, 91.18, 90.97, and 90.94 (internal C≡C), 83.38 (C≡CH), 79.20 (C≡*C*H), 18.82 (CH of TIPS), 11.48 (Me of TIPS); ^{29}Si NMR (79 MHz, $CDCl_3$) δ (ppm) = −1.51.

Preparation of Si-TPE (1; see Scheme 1) by Hydrosilylation of (v). To a degassed solution of 300 mg (0.6 mmol, 1.0 equiv) of (v) in 30 mL of CH_2Cl_2 were added 102 mg of triethoxysilane (0.6 mmol, 1.0 equiv) and 3 drops of Karstedt's catalyst in PDMS (poly(dimethylsiloxane)). After stirring for 48 h the solvent was removed. The resulting dark yellow residue **1** was used without further purification.

^{29}Si NMR (79 MHz, $CDCl_3$) δ (ppm) = −1.65 (TIPS), −57.02 ($Si(OEt)_3$).

Synthesis of the Hybrid Polyoxometalate Species PW_{11}-TPE (3). The lacunary polyoxotungstate $K_7PW_{11}O_{39}$ was synthesized according to known literature.[33] To a dispersion of 670 mg of powdered $K_7PW_{11}O_{39}$ (0.22 mmol, 1.0 equiv) in 700 mL of acetonitrile were added 7.5 equiv of NMe_4Cl (tetramethylammonium chloride, 186 mg, 1.7 mmol), 4.4 equiv of 1 M HCl (1 mmol), and 2.2 equiv of Si-TPE (**1**) (323 mg, 0.5 mmol) in 2 mL of CH_2Cl_2, and the mixture was stirred for 24 h. After filtration, the solvent was removed and the residue was collected. Washing of the residue with water, methanol, and diethyl ether afforded the desired TMA salt of the product as a red powder in 90% yield (810 mg, 0.2 mmol): ^{1}H NMR (400 MHz, DMSO-d_6) δ (ppm) = 8.0−5.5 (very broad, 28H, aromatic and vinylic protons), 3.13 (s, 36H, NMe_4^+), 1.09 (broad, 42H, TIPS); ^{29}Si NMR (79 MHz, MeCN-d_3) δ (ppm) = −1.33 (TIPS), −63.33; ^{31}P NMR (162 MHz, DMSO-d_6) δ (ppm) = −13.60; ^{183}W NMR (25 MHz, DMSO-d_6) δ (ppm) = −97.08 (2W), −101.29 (2W), −106.19 (1W), −119.06 (2W), −195.17 (2W), −245.99 (2W). IR (ATR): 1110 (Si−O−Si), 1064 (P−O), 1054 (P−O), 1035 (P−O), 996, (W═O), 985 (W═O), 959 (W═O), 865 (W−O−W), 806 (W−O−W), 788 (W−O−W) [cm^{-1}]; ESIMS PW_{11}-TPE·DMSO measured m/z = 1265.244 08 (simulation: 1265.229 04); PW_{11}-TPE·2MeCN measured m/z = 1266.590 49 (simulation: 1266.584 78).

Ion Exchange with Na-PW_{11}-TPE. Cations were exchanged with Na^+ by slow filtration of a 5 mg/mL solution of TMA-POM in acetonitrile through a column packed with Amberlite-IR120-Na. The success of the exchange was controlled *via* ^{1}H NMR (no peak at δ = 3.23 ppm any more).

Preparation of High-Concentration Phases. A dispersion of 100 mg of PW_{11}TPE in water was prepared. Acetonitrile was added until full homogenization had taken place. Due to its lower boiling point (82 °C) compared to water, it is removed in a second step slowly under vacuum. The content of water can be controlled by the evaporation time, and its content was investigated using thermogravimetric analysis (TGA).

Analytical Methods. NMR measurements (^{1}H, ^{13}C, ^{29}Si, ^{31}P) were performed on a Varian Unity INOVA 400 spectrometer. The ^{183}W NMR spectra were recorded on a Bruker Avance III 600 MHz spectrometer with 10 mm NMR tubes. ESIMS data were acquired on a Bruker microtof II system. The solutions were injected directly into the evaporation chamber. SAXS was acquired on a Bruker Nanostar system equipped with pinhole collimation and Cu Kα radiation. The samples were placed between X-ray transparent foils and were measured in an evacuated chamber. Liquid samples were sealed in 1 mm Mark tubes made of soda lime glass. TEM was acquired on a Zeiss Libra 120 system and a JEOL JEM-2200FS. The dry sample was placed directly on carbon-coated copper grids. IR spectroscopy was performed on a PerkinElmer 100 system. UV/vis spectroscopy was performed on a Varian Cary 100. Dynamic light scattering was measured on a Viscotek 802 DLS machine. Photosensor measurements were performed on 3 mm × 3 mm sensor substrates from Umweltsensortechnik and measured with a Zahner IM6 potentiostat. A solution of Na-PW_{11}-TPE in acetonitrile/water (5/1) solution was subsequently dropped onto the substrate and allowed to dry. Fluorescence spectroscopy was performed on a FluoTime 3000. All experiments were performed with λ_{ex} = 405 nm. Because signals were too noisy in pure water due to the low concentration of PW_{11}TPE, solutions with higher concentration (c = 5 g/L) were prepared using THF. Cyclic voltammetry was measured with an Epsilon-potentiostat (BASi) (reference electrode: Ag/Ag^+ wire; counter electrode: Pt wire; scan rate: 100 mV/s). Because signals were too noisy in pure water due to the low concentration of PW_{11}TPE, solutions with higher concentration (c = 1 g/L) were prepared using dimethyl sulfoxide (DMSO). TGA was recorded using a Netzsch TG 203 instrument.

ASSOCIATED CONTENT

Supporting Information

The Supporting Information is available free of charge on the ACS Publications website at DOI: 10.1021/acsnano.6b04677.

Additional analytical data (PDF)

AUTHOR INFORMATION

Corresponding Author

*E-mail: sebastian.polarz@hotmail.de.

Author Contributions

A.K. has performed the experiments. S.P. has designed the research and wrote the paper. All authors have given approval to the final version of the manuscript.

Notes

The authors declare no competing financial interest.

ACKNOWLEDGMENTS

The current research was funded by an ERC consolidator grant (I-SURF; project 614606). We thank Prof. R. Winter (University of Konstanz) for assistance with the spectroelectrochemical measurements.

REFERENCES

(1) Ariga, K.; Hill, J. P.; Lee, M. V.; Vinu, A.; Charvet, R.; Acharya, S. Challenges and Breakthroughs in Recent Research on Self-Assembly. *Sci. Technol. Adv. Mater.* **2008**, *9*, 96.

(2) Hirst, A. R.; Escuder, B.; Miravet, J. F.; Smith, D. K. High-Tech Applications of Self-Assembling Supramolecular Nanostructured Gel-Phase Materials: From Regenerative Medicine to Electronic Devices. *Angew. Chem., Int. Ed.* **2008**, *47*, 8002−8018.

(3) Whitesides, G. M.; Grzybowski, B. Self-Assembly at All Scales. *Science* **2002**, *295*, 2418−2421.

DOI: 10.1021/acsnano.6b04677
ACS Nano 2016, 10, 10041−10048

(4) Ozin, G. A.; Hou, K.; Lotsch, B. V.; Cademartiri, L.; Puzzo, D. P.; Scotognella, F.; Ghadimi, A.; Thomson, J. Nanofabrication by Self-Assembly. *Mater. Today* **2009**, *12*, 12−23.
(5) Tschierske, C. Development of Structural Complexity by Liquid-Crystal Self-Assembly. *Angew. Chem., Int. Ed.* **2013**, *52*, 8828−8878.
(6) Hoeben, F. J. M.; Jonkheijm, P.; Meijer, E. W.; Schenning, A. About Supramolecular Assemblies of π-Conjugated Systems. *Chem. Rev.* **2005**, *105*, 1491−1546.
(7) Wang, C. L.; Dong, H. L.; Hu, W. P.; Liu, Y. Q.; Zhu, D. B. Semiconducting π-Conjugated Systems in Field-Effect Transistors: A Material Odyssey of Organic Electronics. *Chem. Rev.* **2012**, *112*, 2208−2267.
(8) Kim, F. S.; Ren, G. Q.; Jenekhe, S. A. One-Dimensional Nanostructures of π-Conjugated Molecular Systems: Assembly, Properties, and Applications from Photovoltaics, Sensors, and Nanophotonics to Nanoelectronics. *Chem. Mater.* **2011**, *23*, 682−732.
(9) McCulloch, I.; Heeney, M.; Bailey, C.; Genevicius, K.; Macdonald, I.; Shkunov, M.; Sparrowe, D.; Tierney, S.; Wagner, R.; Zhang, W. M.; Chabinyc, M. L.; Kline, R. J.; McGehee, M. D.; Toney, M. F. Liquid-Crystalline Semiconducting Polymers with High Charge-Carrier Mobility. *Nat. Mater.* **2006**, *5*, 328−333.
(10) Narayan, R.; Kim, J. E.; Kim, J. Y.; Lee, K. E.; Kim, S. O. Graphene Oxide Liquid Crystals: Discovery, Evolution and Applications. *Adv. Mater.* **2016**, *28*, 3045−3068.
(11) Weiss, E. A. Organic Molecules as Tools To Control the Growth, Surface Structure, and Redox Activity of Colloidal Quantum Dots. *Acc. Chem. Res.* **2013**, *46*, 2607−2615.
(12) Li, W. S.; Yamamoto, Y.; Fukushima, T.; Saeki, A.; Seki, S.; Tagawa, S.; Masunaga, H.; Sasaki, S.; Takata, M.; Aida, T. Amphiphilic Molecular Design as a Rational Strategy for Tailoring Bicontinuous Electron Donor and Acceptor Arrays: Photoconductive Liquid Crystalline Oligothiophene-C(60) Dyads. *J. Am. Chem. Soc.* **2008**, *130*, 8886−7.
(13) Banno, M.; Yamaguchi, T.; Nagai, K.; Kaiser, C.; Hecht, S.; Yashima, E. Optically Active, Amphiphilic Poly(meta-phenylene ethynylene)s: Synthesis, Hydrogen-Bonding Enforced Helix Stability, and Direct AFM Observation of Their Helical Structures. *J. Am. Chem. Soc.* **2012**, *134*, 8718−8728.
(14) Polarz, S.; Landsmann, S.; Klaiber, A. Hybrid Surfactant Systems with Inorganic Constituents. *Angew. Chem., Int. Ed.* **2014**, *53*, 946−954.
(15) Landsmann, S.; Lizandara-Pueyo, C.; Polarz, S. A New Class of Surfactants with Multinuclear, Inorganic Head Groups. *J. Am. Chem. Soc.* **2010**, *132*, 5315−5321.
(16) Giner-Casares, J. J.; Brezesinski, G.; Moehwald, H.; Landsmann, S.; Polarz, S. Polyoxometalate Surfactants as Unique Molecules for Interfacial Self-Assembly. *J. Phys. Chem. Lett.* **2012**, *3*, 322−326.
(17) Landsmann, S.; Luka, M.; Polarz, S. Bolaform Surfactants with Polyoxometalate Head Groups and Their Assembly into Ultra-Small Monolayer Membrane Vesicles. *Nat. Commun.* **2012**, *3*.
(18) Landsmann, S.; Wessig, M.; Schmid, M.; Coelfen, H.; Polarz, S. Smart Inorganic Surfactants: More than Surface Tension. *Angew. Chem., Int. Ed.* **2012**, *51*, 5995−5999.
(19) Klaiber, A.; Landsmann, S.; Loeffler, T.; Polarz, S. Fourfold Action of Surfactants with Superacid Head Groups: Polyoxometalate-Silicone Nanocomposites as Promising Candidates for Proton-Conducting Materials. *New J. Chem.* **2016**, *40*, 919−922.
(20) Brunschwig, B. S.; Creutz, C.; Sutin, N. Optical Transitions of Symmetrical Mixed-Valence Systems in the Class II-III Transition Regime. *Chem. Soc. Rev.* **2002**, *31*, 168−184.
(21) Odobel, F.; Séverac, M.; Pellegrin, Y.; Blart, E.; Fosse, C.; Cannizzo, C.; Mayer, C. R.; Elliott, K. J.; Harriman, A. Coupled Sensitizer−Catalyst Dyads: Electron-Transfer Reactions in a Perylene−Polyoxometalate Conjugate. *Chem. - Eur. J.* **2009**, *15*, 3130−3138.
(22) Xu, B.; Lu, M.; Kang, J.; Wang, D.; Brown, J.; Peng, Z. Synthesis and Optical Properties of Conjugated Polymers Containing Polyoxometalate Clusters as Side-Chain Pendants. *Chem. Mater.* **2005**, *17*, 2841−2851.
(23) Matt, B.; Renaudineau, S.; Chamoreau, L. M.; Afonso, C.; Izzet, G.; Proust, A. Hybrid Polyoxometalates: Keggin and Dawson Silyl Derivatives as Versatile Platforms. *J. Org. Chem.* **2011**, *76*, 3107−3112.
(24) Xu, B.; Wei, Y.; Barnes, C. L.; Peng, Z. Hybrid Molecular Materials Based on Covalently Linked Inorganic Polyoxometalates and Organic Conjugated Systems. *Angew. Chem., Int. Ed.* **2001**, *40*, 2290−2292.
(25) Klaiber, A.; Lanz, C.; Landsmann, S.; Gehring, J.; Drechsler, M.; Polarz, S. Maximizing Headgroup Repulsion: Hybrid Surfactants with Ultrahighly Charged Inorganic Heads and Their Unusual Self-Assembly. *Langmuir* **2016**, *32*, 10920−10927.
(26) Yin, P.; Li, D.; Liu, T. Solution Behaviors and Self-Assembly of Polyoxometalates as Models of Macroions and Amphiphilic Polyoxometalate-Organic Hybrids as Novel Surfactants. *Chem. Soc. Rev.* **2012**, *41*, 7368−83.
(27) Wang, Y.; Weinstock, I. A. Cation Mediated Self-Assembly of Inorganic Cluster Anion Building Blocks. *Dalton Trans.* **2010**, *39*, 6143−6152.
(28) Chaumont, A.; Wipff, G. Interactions between Keggin Anions in Water: The Higher Their Charge, the Higher Their Condensation? A Simulation Study. *Eur. J. Inorg. Chem.* **2013**, *2013*, 1835−1853.
(29) Heeger, A. J. Semiconducting Polymers: The Third Generation. *Chem. Soc. Rev.* **2010**, *39*, 2354−2371.
(30) Birks, J. B. *Photophysics of Aromatic Molecules*; Wiley-Interscience, 1970.
(31) Zimmer, J. P.; Kim, S.-W.; Ohnishi, S.; Tanaka, E.; Frangioni, J. V.; Bawendi, M. G. Size Series of Small Indium Arsenide−Zinc Selenide Core−Shell Nanocrystals and Their Application to In Vivo Imaging. *J. Am. Chem. Soc.* **2006**, *128*, 2526−2527.
(32) Morkoç, H.; Strite, S.; Gao, G. B.; Lin, M. E.; Sverdlov, B.; Burns, M. Large-Band-Gap SiC, III-V Nitride, and II-VI ZnSe-Based Semiconductor-Device Technologies. *J. Appl. Phys.* **1994**, *76*, 1363−1398.
(33) Contant, R. Comparative-Study of Tungstophosphates Related to the $PW_{12}O_{40}^{3-}$ Anion - Synthesis and Properties of $K_{10}P_2W_{20}O_{70}\bullet 24H_2O$, a New Lacunary Polyoxotungstophosphate. *Can. J. Chem.* **1987**, *65*, 568−573.

DOI: 10.1021/acsnano.6b04677
ACS Nano 2016, 10, 10041−10048